

Complementarity of peculiar velocity surveys and redshift space distortions for testing gravity

Alex G. Kim¹ and Eric V. Linder^{1,2,3}

¹*Lawrence Berkeley National Laboratory, Berkeley, California 94720, USA*

²*Berkeley Center for Cosmological Physics, University of California, Berkeley, California 94720, USA*

³*Energetic Cosmos Laboratory, Nazarbayev University, Nur-Sultan 010000, Kazakhstan*



(Received 2 December 2019; published 21 January 2020)

Peculiar-velocity surveys of the low-redshift universe have significant leverage to constrain the growth rate of cosmic structure and test gravity. Wide-field imaging surveys combined with multiobject spectrographs [e.g., ZTF2, Large Synoptic Survey Telescope (LSST), DESI, and 4MOST] can use type Ia supernovae as informative tracers of the velocity field, reaching few percent constraints on the growth rate $f\sigma_8$ at $z \lesssim 0.2$ where density tracers cannot do better than $\sim 10\%$. Combining the high-redshift DESI survey mapping redshift space distortions with a low-redshift supernova peculiar velocity survey using LSST and DESI can determine the gravitational growth index to $\sigma(\gamma) \approx 0.02$, testing general relativity. We study the characteristics needed for the peculiar velocity survey, and how its complementarity with clustering surveys improves when going from a Λ CDM model assumption to a w_0-w_a cosmology.

DOI: [10.1103/PhysRevD.101.023516](https://doi.org/10.1103/PhysRevD.101.023516)

I. INTRODUCTION

The spatial distribution of large scale structure encodes abundant information on the cosmological model. The inhomogeneous clustering is matched by motions—peculiar velocities—with respect to the cosmic expansion, and this also contains important information. These velocities appear, for example, in redshift space distortions (RSD) whose measurement is a major focus of galaxy surveys such as the Dark Energy Spectroscopic Instrument (DESI [1]). However, RSD maps the velocity field in a statistical sense in that velocities are not determined per object but are inferred through the clustering of objects.

One can also seek to measure peculiar velocities directly from individual objects, and then carry out statistical analysis of the velocity field. This, however, requires accurate separation of the cosmic expansion redshift from the measured redshift, which can be accomplished through measured distances and a tight distance-redshift relation. This is generally only practical at low redshifts where the redshift from velocities is not negligible compared to the cosmic redshift. Such peculiar velocity (PV) surveys have employed distance measurements by the fundamental plane relation for elliptical galaxies (e.g., 6dFGS [2,3] and TAIPAN [4,5]), and the Tully-Fisher relation for spiral galaxies (e.g., WALLABY + WNSHS [6]); recently type Ia supernova (SNe Ia) standardized candles have been considered [7–13].

The distance moduli of SNe Ia can be determined relatively precisely, to ~ 0.1 mag as compared to ~ 0.45 mag for Tully-Fisher or Fundamental Plane galaxies. These

translate to proportionate precisions in per-object peculiar velocity. The probative power of a particular probe goes as the distance variance over the number density, so that one SN Ia is worth 20 galaxies. It is only now with current and upcoming SN surveys that the solid-angle coverage and number densities can be competitive with and exceed the performance of galaxy-based peculiar-velocity surveys. In the next decade, the Zwicky Transient Facility (ZTF [14], its proposed successor (ZTF-II), and the Large Synoptic Survey Telescope (LSST) [15] will find $\sim 100,000$ SNe at $z < 0.2$, and DESI and 4MOST [16] can determine accurate redshifts for the host galaxies. With such a number density of distance indicators accurate to perhaps 4%–5% each, the velocity field can be mapped with good signal to noise and the cosmic growth rate $f\sigma_8$ measured to the equivalent of $\sim 3\%$ ([15], this article) in each of two redshift bins at $z = [0, 0.1]$ and $[0.1, 0.2]$ (although there is no need to bin).

This is interesting for cosmology, but especially for testing gravity. That is because the velocity field is an especially robust way to test gravity: density and velocity are simply related by the continuity equation (due to mass conservation), and velocity is proportional to acceleration (in linear perturbation theory) by Euler’s equation for any central force law. Thus these should hold in a wide class of gravity theories. Acceleration is related to density perturbations through Poisson’s equation, and causes the peculiar velocities. Thus peculiar velocities can test the strength of gravity.

In this article we do not assume a particular model of gravity but rather constrain deviations from general

relativity (GR) in terms of the gravitational growth index γ [17]. The growth index is an accurate way of expressing deviations in the growth rate for a wide range of gravity theories, as long as they are scale independent on the scales of interest (linear theory) and do not affect the early Universe initial conditions [18].

Another robust feature of velocity measurements is that the probes (e.g., galaxies) are merely test particles that lie in and map the velocity field sourced by all matter, including dark matter. This is in contrast to overdensity measurements, in which the connection between the baryonic probes (e.g., galaxy light) and dark matter is less direct. Furthermore, velocity surveys complement density surveys by giving more weight on larger scales (smaller Fourier wave numbers k) and the two together can at least partially cancel sample variance.

This article expands on previous work by exploring the complementarity of low-redshift SN-based peculiar velocity measurements with higher-redshift RSD measurements of DESI in probing gravity. These data sets give it a lever arm spanning the broad redshift range $0 < z < 2$, and we focus on the gravitational growth index γ as an indicator of deviations from general relativity, and a measure of stronger or weaker gravity.

In Sec. II we briefly summarize the survey characteristics and method of using the peculiar velocity power spectrum (and cross-correlation with the matter density power spectrum) to constrain cosmological parameters. We present the results on γ and other parameters in Sec. III, especially the complementarity with higher redshift RSD surveys. We conclude in Sec. IV.

II. SURVEYS AND METHOD

The properties of peculiar velocity surveys that most strongly determine their sensitivity to the growth of structure are as follows:

- (i) The survey volume: We assume a volume of the shape of a shell defined by its minimum (r_{\min}) and maximum (r_{\max}) radial distances, and its solid angle (Ω). At small galaxy separations, observed redshifts can be dominated by peculiar rather than cosmological redshifts, a regime that is not well described by linear theory: we thus adopt an r_{\min} that corresponds to $z_{\min} = 0.01$. While source detections are generally based on source magnitude, for convenience we set $z_{\max} = 0.2$ up to which complete SN Ia telescope follow-up is reasonable and beyond which large velocity uncertainties limit the precision in measuring the growth of structure. We consider that to cover half of the extragalactic sky, $\Omega = 2\pi$, using both northern and southern hemisphere resources.
- (ii) Number density of the probes n : While different classes of object may be used as density and velocity probes, in this article we consider one class used for both. For transient probes such as SNe Ia, the density

is directly related to the survey duration. We consider a 10-year survey with 0.65 efficiency and a SN-frame rate of $2.69 \times 10^{-5} (h/0.70)^3 \text{ Mpc}^{-3} \text{ yr}^{-1}$ [19]. A constant rate is adopted for the $z < 0.2$ volume considered in this article; the slow increase in observer-frame rate with redshift is dwarfed by the corresponding increase in velocity uncertainty described in the next paragraph.

- (iii) σ_M : Intrinsic magnitude dispersion of the probe: A fixed magnitude dispersion transforms into a distance-dependent velocity dispersion σ through $\sigma_M^2 = \left(\frac{5}{\ln 10}\right)^2 \left(1 - \frac{1}{aH\chi}\right)^2 \sigma^2$, where χ is the comoving distance. We consider a value of $\sigma_M = 0.08 \text{ mag}$ [20–23] that could be achieved using data beyond optical photometry. Here, σ_M is the intrinsic magnitude dispersion and redshift independent; i.e., the surveys are designed to have subdominant measurement uncertainties over all redshifts. The velocity dispersion σ increases with increasing redshift (proportional to z at low redshift) reducing the probative power of distance indicators with increasing distance.

We add to σ in quadrature $\sigma_v = 300 \text{ km s}^{-1}$ as an uncorrelated per-object random uncertainty caused by short-scale nonlinear effects not captured by our model. This limits the probative power at the lowest redshifts. For our choice of σ_M and background cosmology, $\sigma = \sigma_v$ at $z = 0.026$.

- (iv) Range of k included in the analysis: k_{\min} and k_{\max} are set respectively according to the linear extent of the survey volume and the smallest scales that are confidently modeled. We use $k_{\min} = (\pi/r_{\max})h/\text{Mpc}$ and $k_{\max} = 0.1h/\text{Mpc}$.

A cosmological model predicts the statistical properties of the spatial distribution and line-of-sight velocities of the probe through the density-density ($P_{\delta\delta}$), velocity-velocity (P_{vv}), and the cross density-velocity ($P_{\delta v}$) power spectra. In linear perturbation theory, the dark-matter overdensity field can be decomposed into independent temporal and spatial components, where the temporal component $D(t)$ is known as the growth function. The galaxy overdensity is taken to be proportional to that of dark matter with a bias factor b . To first order, the galaxy power spectrum in the observed redshift space is proportional to the dark-matter power spectrum in real space as $P_{\delta\delta} \propto (bD + fD\mu^2)^2 P_{mm}$ [24]. Dark-matter densities and velocities of test particles are related through the continuity equation as $P_{vv} \propto (fD\mu)^2 P_{mm}$ [25]. The galaxy-velocity cross-correlation is then $P_{v\delta} \propto (bD + fD\mu^2) fD\mu$ [26]. In the above $f = d \ln D / d \ln a$ and μ is the cosine of the angle between the observers line of sight and the k -space vector. Note that the commonly used mass fluctuation amplitude σ_8 is proportional to D .

We consider two approaches to extracting cosmological information from the power spectra. For the first approach,

fD is taken to have constant, independent values in a set of redshift bins, and bD is taken to have a constant value over all redshift bins (stable clustering). The parameter set is then $\lambda \in \{fD_1, \dots, fD_{n_b}, bD\}$ for n_b redshift bins. This model is commonly used to project and report the results of peculiar velocity surveys [27].

The second approach puts the focus on gravity. References [17,18] found that $f = \Omega_m(a)^\gamma$ provides a highly accurate ($\lesssim 0.3\%$) description of the growth of structure, where a wide range of gravity models can be described by single values of the growth index γ . The mass density in units of the critical density, $\Omega_m(a)$, itself depends on cosmological parameters describing the background expansion; for this article we consider a flat cosmology with the standard $w(a) = w_0 + w_a(1-a)$ dark energy equation of state. The bias b is taken to be constant in the narrow $0 < z < 0.2$ redshift range. The density and velocity covariances then depend on the parameter set $\lambda \in \{\gamma, \Omega_m, w_0, w_a, b\}$, where Ω_m (without an argument) is the mass density today.

We project parameter uncertainties¹ using the Fisher information matrix

$$F_{ij} = \frac{\Omega}{8\pi^2} \int_{r_{\min}}^{r_{\max}} dr \int_{k_{\min}}^{k_{\max}} dk \int_{-1}^1 d\mu r^2 k^2 \text{Tr} \left[C^{-1} \frac{\partial C}{\partial \lambda_i} C^{-1} \frac{\partial C}{\partial \lambda_j} \right], \quad (1)$$

where

$$C(k, \mu, a) = \begin{bmatrix} P_{\delta\delta}(k, \mu, a) + \frac{1}{n} & P_{v\delta}(k, \mu, a) \\ P_{v\delta}(k, \mu, a) & P_{vv}(k, \mu, a) + \frac{\sigma^2 + \sigma_v^2}{n} \end{bmatrix}. \quad (2)$$

The fiducial cosmology is a Λ CDM model ($w_0 = -1$, $w_a = 0$), with $\Omega_m = 0.3$, and a power spectrum calculated by CAMB [28] using its default configuration.

For the calculations in this article we use the SN galaxy hosts as the density (δ) probe at $z < 0.2$, as in [15]. The addition of other survey galaxies in this redshift range results in only small improvement in parameter estimation (for example, the DESI Bright Galaxy Survey galaxies have a precision on $f\sigma_8$ exceeding 10%, compared to the $\sim 2\%$ here). Most of the probative power at $z < 0.2$ comes from peculiar velocities, with the covariance of the density measurement providing only a slight decrease in the sample-variance floor (see Fig. 2 in [13]).

III. RESULTS TESTING GRAVITY

From the peculiar velocity survey we have measurements of $f\sigma_8$ over $0.01 < z < 0.2$. We can compare or combine these with measurements of redshift space

¹The code is available at <https://github.com/LSSTDESC/SNPeculiarVelocity>.

distortions from DESI. The precisions that DESI are expected to deliver are listed in Tables 2.3 and 2.5 of [1], where we use the full redshift range. Since our main goal here is testing gravity, we only use its $f\sigma_8$ measurements (with $k_{\max} = 0.1h/\text{Mpc}$), not the baryon acoustic oscillation measurements. We also emphasize that DESI provides far more cosmological leverage than the growth index γ constraints we focus on here; in particular, measuring the cosmic growth history over a wide range of redshift as DESI does is highly fundamental and insightful.

To motivate why low-redshift surveys can be competitive with the huge volumes of high-redshift surveys for the particular goal of measuring γ , note that as one approaches the matter dominated era the growth rate f approaches unity. Since γ is defined through $f = \Omega_m(a)^\gamma$, γ is relatively poorly determined as $\Omega_m(a) \rightarrow 1$ at higher redshifts. Since $f\sigma_8 \propto fD$ and $D/a \rightarrow 1$ (appropriately normalized) at higher redshifts, the insensitivity to γ is compounded. However, at low redshift, both f and D/a deviate from unity and γ has increased influence, making low-redshift measurements of $f\sigma_8$ a good avenue for testing whether γ is consistent with its general relativity value of 0.55.

Figure 1 illustrates this, plotting $f\sigma_8(z)$ for various values of γ , relative to the general relativity behavior for the same background cosmology. The curves flare out at low redshift, pointing to an opportunity there if the measurement precision can be made reasonable. Overplotted are the expected measurement uncertainties

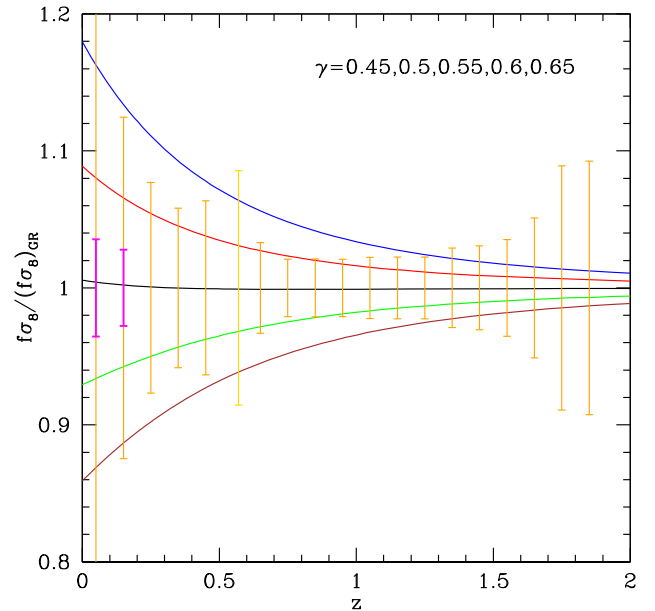


FIG. 1. The ratio of the growth rate $f\sigma_8$ to the GR behavior is plotted for five values of the gravitational growth index γ , increasing from top to bottom. Note that $\gamma = 0.55$ is a highly accurate approximation to GR. DESI RSD (medium orange), current baryon oscillation spectroscopic survey RSD (lighter gold), and peculiar velocity survey (dark magenta) uncertainties in 0.1 redshift bins are overplotted.

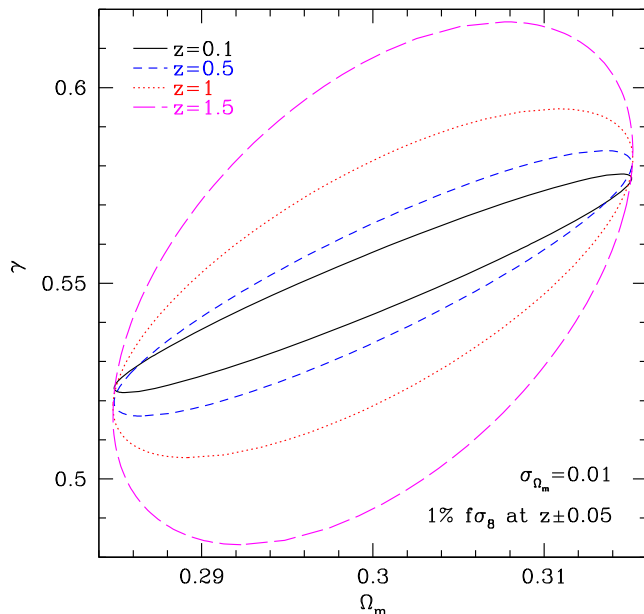


FIG. 2. Low-redshift measurements of the growth rate $f\sigma_8$ give improved constraints in the Ω_m - γ plane. Relative to higher redshift, $z \approx 0.1$ measurements give tighter confidence contours and ones oriented more narrowly in the γ axis. This plot is for illustrative 1% measurements of $f\sigma_8$ at $z \pm 0.05$ in a Λ CDM universe, combined with a Gaussian prior of 0.01 on Ω_m , at four different redshifts z .

on $f\sigma_8$ in redshift bins of width 0.1 from the DESI RSD in the main survey (above $z > 0.6$), from the DESI RSD in the Bright Galaxy Survey (below $z < 0.5$), and our baseline peculiar velocity survey, using the first approach of Sec. II.

While the γ curves for $f\sigma_8(z)$ give a useful indication of the strength of deviations from general relativity for a given γ , the observational constraints on γ also depend on covariance with other cosmological parameters such as the matter density Ω_m (recall that γ , by construction [17], has relatively little covariance with the dark energy equation of state parameters, and this is especially true at low redshift). The same advantages of low-redshift measurements still hold, demonstrated in Fig. 2 with the joint confidence contours on γ and Ω_m . This gives a feel for the sensitivity of measurements near particular redshifts, by adopting simply a localized pair of measurements at $z \pm 0.05$. (A Gaussian prior of 0.01 on Ω_m is included for convenience in drawing reasonable confidence contours from only two measurements; we have checked that this does not substantially alter the degeneracy direction.)

Keeping the measurement precision fixed (at 1% for purely illustrative purposes), high-redshift measurements of $f\sigma_8$ have less constraining power on γ than low-redshift ones. Furthermore, the degeneracy direction of the contours slowly rotates with the measurement redshift, becoming more favorable with respect to determining γ at low redshift. The general degeneracy direction is simple to understand: increasing Ω_m increases growth, while

increasing γ (essentially decreasing the strength of gravity; see [18]) decreases growth. Thus doing both compensates for each, extending the contour along the positive slope diagonal. At high redshift, since the measurement is less sensitive to γ , a given change in Ω_m requires a larger change in γ , steepening the slope and rotating the contour counter-clockwise; for low redshift, the opposite occurs and the clockwise-rotated contour gives tighter constraints on γ .

Having established that low-redshift peculiar velocity surveys have the potential to help test gravity, we carry out a full Fisher information matrix analysis of the cosmological and gravity parameter constraints (using the second approach of Sec. II and so without any need to bin measurements of $f\sigma_8$) enabled by the baseline PV survey of Sec. II, and also that combined with DESI RSD measurements. We consider two cosmological models: Λ CDM characterized by the matter density Ω_m , and dynamical dark energy characterized by Ω_m and the dark energy parameters w_0 and w_a describing its present equation of state and its time variation. In addition there is the gravitational growth index γ (and source bias parameter, which is always marginalized over). To roughly represent other cosmological data besides PV and RSD in the DESI-LSST era, we impose a Gaussian prior on Ω_m of width 0.01.

We find that in the Λ CDM model, PV alone determines γ to 0.020 and RSD alone to 0.026. That is, within this

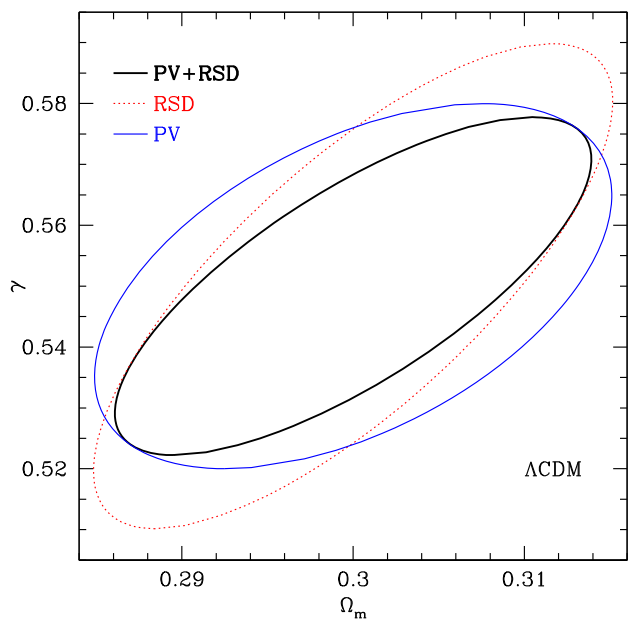


FIG. 3. PV measurements from our fiducial survey at $z = 0-0.2$ give comparable constraints (contours at the 1σ joint confidence level) in the Ω_m - γ plane to DESI RSD measurements over $z = 0-1.8$. (Of course DESI gives crucial information on the whole growth history, not merely its compression into Ω_m - γ .) The combination of the two surveys gives further improvement. Here Λ CDM is assumed.

limited focus on testing gravity in the form of γ (which indeed provides a subpercent accurate fit to the effect of many modified-gravity models on cosmic growth in the linear regime), low-redshift PV can match DESI RSD. Combining the two yields an improvement to $\sigma(\gamma) = 0.018$. Recall that the distance in γ between general relativity and $f(R)$ gravity or braneworld gravity is ± 0.13 respectively and a key science goal of the Euclid dark energy satellite mission is testing γ to 0.02.

Figure 3 shows the 1σ joint confidence contours in the Ω_m - γ plane for these cases. We see that the two-dimensional joint confidence contours of PV and RSD are complementary, and the “figure of merit” (FOM; inverse area in terms of the inverse square root of the determinant of the Ω_m - γ covariance matrix) of the combined confidence region improves by 1.5/1.5 times relative to the individual probes, respectively.

However, when we allow more cosmological freedom as in the w_0 - w_a model, the situation is different. The constraints become $\sigma(\gamma) = 0.15$ for DESI RSD but 0.029 for PV + RSD; i.e., peculiar velocities play a crucial role in testing gravity when there is also freedom in the nature of dark energy. Essentially, the PV survey together with the RSD survey allows simultaneous fitting of Ω_m , w_0 , w_a , and γ with reasonable constraints.

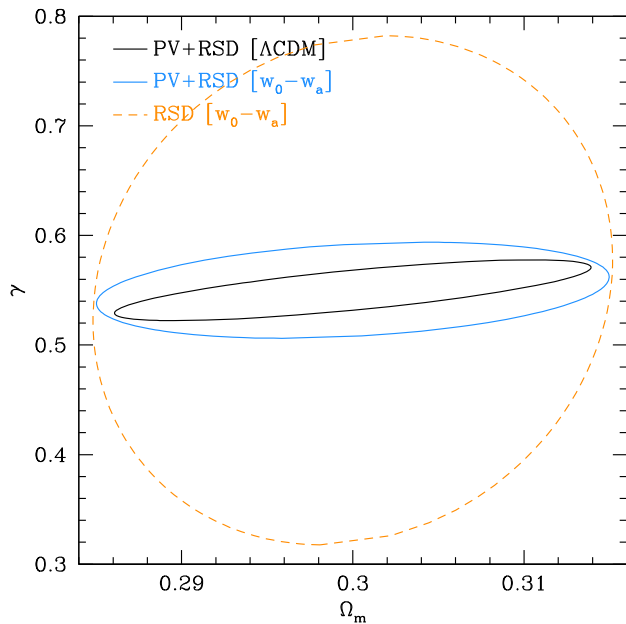


FIG. 4. The same as Fig. 3, but with marginalizing over the dark energy equation of state parameters w_0 , w_a rather than fixing to Λ CDM. Note, the complementarity between peculiar velocities and redshift space distortions keeps the constraints from weakening too much when also fitting for w_0 and w_a (solid light blue RSD + PV contour vs the solid black contour fixed to Λ CDM and the same as in Fig. 3). However, the confidence contour using RSD alone (dashed orange) blows up considerably in going from a Λ CDM to w_0 - w_a model.

TABLE I. Summary of constraints on the gravitational growth index γ and the FOM ($1/\sqrt{\det COV[\Omega_m, \gamma]}$) for various cosmology models and data sets. PV is the low-redshift peculiar velocity survey; RSD is the DESI redshift space distortions. We show both the baseline case of using modes out to $k_{\max} = 0.1h/\text{Mpc}$ and the optimistic case with $0.2h/\text{Mpc}$. All cases include a prior of $\sigma(\Omega_m) = 0.01$.

Model	Data	$k_{\max} = 0.1$		$k_{\max} = 0.2$	
		$\sigma(\gamma)$	FOM	$\sigma(\gamma)$	FOM
Λ CDM	PV	0.0198	5862	0.0160	7934
Λ CDM	RSD	0.0262	5891	0.0214	12267
Λ CDM	PV + RSD	0.0183	9037	0.0156	17627
$w_0 - w_a$	PV	0.0767	1315	0.0555	1834
$w_0 - w_a$	RSD	0.153	659	0.0707	1467
$w_0 - w_a$	PV + RSD	0.0289	3654	0.0203	5531

Figure 4 shows that RSD alone has difficulty fitting all the parameters together, but adding PV substantially immunizes against this issue, still allowing reasonable constraints. Now the figure of merit improvement in the Ω_m - γ plane for the combined probes is a factor of 2.8/5.5 respectively relative to PV/RSD alone. Alternately, one could say that allowing going beyond a Λ CDM background blows up the Ω_m - γ contour for RSD alone by a factor 8.9, but increases the area for PV + RSD by only a factor 2.5, as shown by the black contour going to the blue one.

If modeling allows accurate use of modes out to $k_{\max} = 0.2h/\text{Mpc}$ instead, then the combination of PV + RSD can determine γ to 0.016 (0.020) in the Λ CDM (w_0 - w_a) cosmology case. The figure of merit improvement in the Ω_m - γ plane with the higher k_{\max} is a factor of 2.0 (1.5). All the results are summarized in Table I.

IV. CONCLUSIONS

Peculiar velocities provide a direct measurement of the growth of structure, and hence serve as a powerful probe of the gravitational forces responsible for the clustering and motion within the expanding Universe. At low redshift, peculiar velocities can be measured from individual galaxies whose distances are accurately measured, e.g., through type Ia supernovae. At high redshift, the imprint of peculiar velocities creates a specific anisotropy in the correlation functions of the redshift-space coordinates of ensembles of galaxies.

Each approach can provide constraints on the growth index γ that can distinguish classes of gravity. A distinguishing feature of direct peculiar velocities is that precise measurements are confined to low redshift, but here the sensitivity to γ “flares” in enhancement, while higher redshift RSD measurements are more sensitive to Ω_m than γ [since as $\Omega_m(a) \rightarrow 1$, γ is poorly determined]. The two methods therefore have great complementarity in testing gravity. This advantage strengthens further when $\Omega_m(a)$ becomes more flexible in models that go beyond Λ CDM.

The upcoming generation of redshift and transient object surveys gives exciting data sets that can be used in these ways. Cadenced multiband imaging surveys such as ZTF-2 and LSST can provide near-full sky, complete low-redshift SN discoveries and light curves used to obtain host distances. Wide-field multiobject spectrographs such as DESI and 4MOST can follow up these discoveries to get multiplexed transient classifications and redshifts; the use of these instruments for peculiar velocities is being considered by the DESI Collaboration and in the 4MOST Hemisphere Survey proposal. Other 2–4m class facilities can provide supplemental near infrared and spectroscopic data to improve the data set [29,30]. A coordinated effort is required to organize the diverse range of facilities that comprise a complete peculiar-velocity survey.

Improvements in the absolute-magnitude calibration of SNe Ia hone the probative power of each individual object. In this article, we adopt a 0.08 mag intrinsic dispersion achieved with SN samples with supplemental data beyond optical light curves [20–23]. The relationship between σ_M and $\sigma(\gamma)$, plotted in [13], is nontrivial as both sample variance and shot noise contribute to the error budget in the survey we consider.

We projected cosmology and gravity constraints with two approaches, using $f\sigma_8$ and going directly to the gravitational growth index γ . The Fisher code for dealing with peculiar velocity surveys is publicly available. The results highlight the significant complementarity between peculiar velocity and redshift space distortion surveys, especially as the dark energy properties are fit simultaneously. Testing gravity with $\sigma(\gamma) \approx 0.02$ appears achievable. Further improvements are possible if our understanding of perturbation theory allows use of smaller scale modes, with figure of merit increases of 1.5–2. Any sign of deviation of the value of γ from general relativity would then motivate more detailed analysis with more sophisticated tests of how gravity behaves on cosmic scales.

ACKNOWLEDGMENTS

We thank Arman Shafieloo and KASI for hospitality during part of this work and Yong-Seon Song for helpful conversations. This work is supported in part by the U.S. Department of Energy, Office of Science, Office of High Energy Physics, under Award No. DE-SC-0007867 and Contract No. DE-AC02-05CH11231, and by the Energetic Cosmos Laboratory.

-
- [1] A. Aghamousa, J. Aguilar, S. Ahlen, S. Alam, L. E. Allen *et al.* (DESI Collaboration), The DESI experiment part I: Science, targeting, and survey design, [arXiv:1611.00036](https://arxiv.org/abs/1611.00036).
 - [2] D. Burkey and A. N. Taylor, Prospects for galaxy-mass relations from the 6dF Galaxy Survey, *Mon. Not. R. Astron. Soc.* **347**, 255 (2004).
 - [3] C. Adams and C. Blake, Improving constraints on the growth rate of structure by modelling the density-velocity cross-correlation in the 6dF Galaxy Survey, *Mon. Not. R. Astron. Soc.* **471**, 839 (2017).
 - [4] J. Koda, C. Blake, T. Davis, C. Magoulas, C. M. Springob, M. Scrimgeour, A. Johnson, G. B. Poole, and L. Staveley-Smith, Are peculiar velocity surveys competitive as a cosmological probe?, *Mon. Not. R. Astron. Soc.* **445**, 4267 (2014).
 - [5] E. da Cunha, A. M. Hopkins, M. Colless, E. N. Taylor, C. Blake *et al.*, The Taipan Galaxy Survey: Scientific goals and observing strategy, *Pub. Astron. Soc. Aust.* **34**, e047 (2017).
 - [6] S. Johnston, R. Taylor, M. Bailes, N. Bartel, C. Baugh *et al.*, Science with ASKAP: The Australian square-kilometre-array pathfinder, *Exp. Astron.* **22**, 151 (2008).
 - [7] C. Gordon, K. Land, and A. Slosar, Cosmological Constraints from Type Ia Supernovae Peculiar Velocity Measurements, *Phys. Rev. Lett.* **99**, 081301 (2007).
 - [8] A. Abate and O. Lahav, The three faces of Ω_m : Testing gravity with low- and high-redshift SNe Ia surveys, *Mon. Not. R. Astron. Soc.* **389**, L47 (2008).
 - [9] A. Johnson, C. Blake, J. Koda, Y.-Z. Ma, M. Colless, M. Crocce, T. M. Davis, H. Jones, C. Magoulas, J. R. Lucey, J. Mould, M. I. Scrimgeour, and C. M. Springob, The 6dF Galaxy Survey: Cosmological constraints from the velocity power spectrum, *Mon. Not. R. Astron. Soc.* **444**, 3926 (2014).
 - [10] D. Huterer, D. L. Shafer, and F. Schmidt, No evidence for bulk velocity from type Ia supernovae, *J. Cosmol. Astropart. Phys.* **12** (2015) 033.
 - [11] T. Castro, M. Quartin, and S. Benitez-Herrera, Turning noise into signal: Learning from the scatter in the Hubble diagram, *Phys. Dark Universe* **13**, 66 (2016).
 - [12] D. Huterer, D. L. Shafer, D. M. Scolnic, and F. Schmidt, Testing Λ CDM at the lowest redshifts with SN Ia and galaxy velocities, *J. Cosmol. Astropart. Phys.* **5** (2017) 015.
 - [13] A. Kim, G. Aldering, P. Antilogus, A. Bahmanyar, S. BenZvi *et al.*, Testing gravity using type Ia supernovae discovered by next-generation wide-field imaging surveys, *Bull. AAS* **51**, 140 (2019), [arXiv:1903.07652](https://arxiv.org/abs/1903.07652).
 - [14] E. C. Bellm, S. R. Kulkarni, M. J. Graham, R. Dekany, R. M. Smith *et al.*, The Zwicky Transient Facility: System overview, performance, and first results, *Publ. Astron. Soc. Pac.* **131**, 018002 (2019).
 - [15] C. Howlett, A. S. G. Robotham, C. D. P. Lagos, and A. G. Kim, Measuring the growth rate of structure with type Ia supernovae from LSST, *Astrophys. J.* **847**, 128 (2017).
 - [16] E. Swann, M. Sullivan, J. Carrick, S. Hoenig, I. Hook, R. Kotak, K. Maguire, R. McMahon, R. Nichol, and S. Smartt,

- 4MOST consortium survey 10: The time-domain extragalactic survey (TiDES), *The Messenger* **175**, 58 (2019).
- [17] E. V. Linder, Cosmic growth history and expansion history, *Phys. Rev. D* **72**, 043529 (2005).
- [18] E. V. Linder and R. N. Cahn, Parameterized beyond-Einstein growth, *Astropart. Phys.* **28**, 481 (2007).
- [19] B. Dilday, M. Smith, B. Bassett, A. Becker, R. Bender *et al.*, Measurements of the rate of type Ia supernovae at redshift $\lesssim 0.3$ from the Sloan Digital Sky Survey II supernova survey, *Astrophys. J.* **713**, 1026 (2010).
- [20] R. L. Barone-Nugent, C. Lidman, J. S. B. Wyithe, J. Mould, D. A. Howell *et al.*, Near-infrared observations of Type Ia supernovae: The best known standard candle for cosmology, *Mon. Not. R. Astron. Soc.* **425**, 1007 (2012).
- [21] C. R. Burns, M. Stritzinger, M. M. Phillips, E. Y. Hsiao, C. Contreras, S. E. Persson, G. Folatelli, L. Boldt, A. Campillay, S. Castellón, W. L. Freedman, B. F. Madore, N. Morrell, F. Salgado, and N. B. Suntzeff, The Carnegie Supernova Project: Intrinsic colors of type Ia supernovae, *Astrophys. J.* **789**, 32 (2014).
- [22] H. K. Fakhouri, K. Boone, G. Aldering, P. Antilogus, C. Aragon *et al.*, Improving cosmological distance measurements using twin type Ia supernovae, *Astrophys. J.* **815**, 58 (2015).
- [23] V. Stanishev, A. Goobar, R. Amanullah, B. Bassett, Y. T. Fantaye, P. Garnavich, R. Hlozek, J. Nordin, P. M. Okouma, L. Östman, M. Sako, R. Scalzo, and M. Smith, Type Ia supernova Hubble diagram with near-infrared and optical observations, *Astron. Astrophys.* **615**, A45 (2018).
- [24] N. Kaiser, Clustering in real space and in redshift space, *Mon. Not. R. Astron. Soc.* **227**, 1 (1987).
- [25] Y.-Z. Ma, C. Gordon, and H. A. Feldman, Peculiar velocity field: Constraining the tilt of the Universe, *Phys. Rev. D* **83**, 103002 (2011).
- [26] Y.-S. Song and W. J. Percival, Reconstructing the history of structure formation using redshift distortions, *J. Cosmol. Astropart. Phys.* **10** (2009) 004.
- [27] C. Howlett, L. Staveley-Smith, and C. Blake, Cosmological forecasts for combined and next-generation peculiar velocity surveys, *Mon. Not. R. Astron. Soc.* **464**, 2517 (2017).
- [28] A. Lewis and S. Bridle, Cosmological parameters from CMB and other data: A Monte Carlo approach, *Phys. Rev. D* **66**, 103511 (2002).
- [29] B. Lantz, G. Aldering, P. Antilogus, C. Bonnaud, L. Capoani, A. Castera, Y. Copin, D. Dubet, E. Gangler, F. Henault, J.-P. Lemonnier, R. Pain, A. Pecontal, E. Pecontal, and G. Smadja, SNIFS: A wideband integral field spectrograph with microlens arrays, *Proc. SPIE Int. Soc. Opt. Eng.* **5249**, 146 (2004).
- [30] M. Rigault, The SEDMachine: Automatic observations and classifications of ZTF Transients, in *The Extragalactic Explosive Universe: The New Era of Transient Surveys and Data-Driven Discovery* (2019), p. 42, <https://doi.org/10.5281/zenodo.3478078>.